



OPEN

SUBJECT AREAS:

ENVIRONMENTAL
MICROBIOLOGY

BACTERIAL GENOMICS

Genomic and metabolic analysis of
fluoranthene degradation pathway in
Celeribacter indicus P73^TJunwei Cao^{1,2*}, Qiliang Lai^{1*}, Jun Yuan¹ & Zongze Shao¹Received
16 July 2014Accepted
20 November 2014Published
13 January 2015Correspondence and
requests for materials
should be addressed to
Z.S. (shaozz@163.
com)* These authors
contributed equally to
this work.

¹State Key Laboratory Breeding Base of Marine Genetic Resources; Key Laboratory of Marine Genetic Resources, The Third Institute of State Oceanic Administration; Key Laboratory of Marine Genetic Resources of Fujian Province; Collaborative Innovation Center of Deep Sea Biology; Collaborative Innovation Center for Exploitation and Utilization of Marine Biological Resources, Xiamen 361005, China, ²School of Municipal and Environmental Engineering, Harbin Institute of Technology, Harbin 150090, China.

Celeribacter indicus P73^T, isolated from deep-sea sediment from the Indian Ocean, is capable of degrading a wide range of polycyclic aromatic hydrocarbons (PAHs) and is the first fluoranthene-degrading bacterium within the family *Rhodobacteraceae*. Here, the complete genome sequence of strain P73^T is presented and analyzed. Besides a 4.5-Mb circular chromosome, strain P73^T carries five plasmids, and encodes 4827 predicted protein-coding sequences. One hundred and thirty-eight genes, including 14 dioxygenase genes, were predicted to be involved in the degradation of aromatic compounds, and most of these genes are clustered in four regions. P73_0346 is the first fluoranthene 7,8-dioxygenase to be discovered and the first fluoranthene dioxygenase within the toluene/biphenyl family. The degradative genes in regions B and D in P73^T are absent in *Celeribacter baekdonensis* B30, which cannot degrade PAHs. Four intermediate metabolites [acenaphthylene-1(2H)-one, acenaphthenequinone, 1,2-dihydroxyacenaphthylene, and 1,8-naphthalic anhydride] of fluoranthene degradation by strain P73^T were detected as the main intermediates, indicating that the degradation of fluoranthene in P73^T was initiated by dioxygenation at the C-7,8 positions. Based on the genomic and metabolitic results, we propose a C-7,8 dioxygenation pathway in which fluoranthene is mineralized to TCA cycle intermediates.

Polycyclic aromatic hydrocarbons (PAHs) are ubiquitous, toxic, and persistent organic compounds in the environment. Microbial degradation studies have shown that biodegradation of PAHs is an efficient way to remove these pollutants from the environment¹. Microorganisms can produce a number of catabolic enzymes and have developed different mechanisms to degrade PAHs. The degradation of PAH is usually initiated by hydroxylation, especially dioxygenation, which is catalyzed by oxygenase². PAHs are then transformed through different peripheral pathways into a few key intermediates (such as protocatechuate, salicylate, gentisate, and catechol), which subsequently are metabolized via the central pathways^{2,3}. Metabolic pathways have been proposed in many degraders; for example, *Mycobacterium vanbaalenii* PYR-1^{2,4}, *Mycobacterium* sp. JS14⁵, *Sinorhizobium* sp. C4⁶, *Sphingomonas* sp. LB126⁷, *Rhodococcus* spp.⁸, *Pasteurella* sp. IFA⁹, *Staphylococcus* sp. PN/Y¹⁰, *Burkholderia fungorum* LB400¹¹ and *Pseudomonas* sp. PP2¹², but rarely in marine bacteria. Although great advances have been made, many aspects of PAH biodegradation, especially of high-molecular-weight PAHs, remain unclear.

Fluoranthene, a non-alternant high-molecular-weight PAH, that contains a five-member ring, is structurally similar to other compounds of environmental concern, such as acenaphthylene, carbazole, fluorene, dibenzodioxin, dibenzofuran, and dibenzothiophene^{1,4}. Therefore fluoranthene has been used as a model compound for biodegradation studies, and many bacterial fluoranthene degraders have been reported; for example, bacteria in the genera *Sphingomonas*¹³, *Alcaligenes*¹⁴, *Burkholderia*¹⁵, *Pseudomonas*¹⁶, *Mycobacterium*^{5,17,18} and *Rhodococcus*¹⁹. However, only a few fluoranthene degraders belonging to the genera *Ochrobactrum*²⁰, *Novosphingobium*²¹, *Cycloclasticus*²², and *Celeribacter*²³ have been isolated from the marine environment. Fluoranthene degradation was found to be initiated by dioxygenation at the C-1,2, C-2,3 C-7,8, and C-8,9 positions^{4,5,9,17,18,24} or a possible monooxygenation to produce monohydroxyfluoranthene⁷. Despite these advances, gaps in our knowledge of the mechanisms of fluoranthene degradation still exist, especially for marine-sourced degraders.



Complete genome sequencing can provide more information, including possible insights into the mechanisms of aromatic compounds degradation, and a large number of PAH-degraders have been sequenced. For example, the *Mycobacterium vanbaalenii* PYR-1 genome was reported with focus on the aromatic catabolic genes in the PAH pathway²⁵. The phenanthrene-degrading bacterium *Delftia* sp. Cs1-4 harbors a novel genomic island, *phn* island, containing genes in the PAH catabolic pathway²⁶. Comparative genomic analyses of the marine bacterium *Alteromonas* sp. SN2 revealed that genetic acquisitions contributed to its ability to metabolize PAHs²⁷. The genome of *Polaromonas naphthalenivorans* CJ2 was reported to contain genes for at least four central pathways and numerous peripheral pathways for aromatic compound metabolism²⁸. However, research on the mechanism of PAH degradation is far to be understood, many aspects of the metabolic pathways remain unknown.

Celeribacter indicus P73^T (=MCCC 1A01112^T =LMG 27600^T =DSM 27257^T), isolated from deep-sea sediment from the Indian Ocean by enrichment of PAHs, was shown to be able to degrade a wide range of PAHs, including naphthalene, phenanthrene, dibenzothiophene, and fluoranthene²³. Strain P73^T is the first fluoranthene-degrading bacterium to be found within the family *Rhodobacteraceae*. Here we report the complete genome sequence of *C. indicus* P73^T with the focus on the aromatic degradative genes involved in the metabolism of PAHs, and describe a possible fluoranthene degradation pathway in strain P73^T.

Results

General aspects of the P73^T genome. The complete genome sequence of *C. indicus* P73^T was 4,969,388-bp long, comprising a circular chromosome of 4,529,105 bp and five plasmids ranging from 7053 bp to 155,183 bp in length (Figure 1 and Table 1). The complete genome had a G + C content of 65.74 mol%, and contained 4827 predicted protein-coding sequences (CDSs) with an average length of 909 bp, giving a coding density of 88.30%. Among the 4827 CDSs, 3908 (80.96%) were assigned to 22 different clusters of orthologous groups (COGs) (see Supplementary Text S1 and Supplementary Data S1 for details). The chromosome encodes two sets of rRNA genes (two 5S rRNA, two 16S rRNA, and two 23S rRNA), 48 tRNA genes with 42 different anticodons that represent only 19 amino acids, and a tRNA for OTHER amino acid. No gene for tRNA-Tyr was found, although the corresponding tyrosyl-tRNA synthetase gene (P73_1712) was identified.

Thirty-seven GIs (36 in the chromosome, one in plasmid pP73C) were predicted in the genome of strain P73^T by SIGI-HMM using IslandViewer²⁹, comprising a total of 314,694-bp (6.33% of the genome) and 346 predicted CDSs (see Supplementary Text S2, Supplementary Figure S1 and Supplementary Data S2 for details). Seven hundred and forty nine horizontally transferred genes (HTG) in the P73^T genome were identified against the genomes of other bacteria in the IMG database (24 October 2013), most of which (56.6%, 424/749) had best hits to HTG from order *Rhizobiales*. Genes involved in PAH degradation were found among these HTG suggesting that strain P73^T may have used gene transfer to enhance its PAH degradation ability (see Supplementary Text S3 and Supplementary Data S3 for details).

Strain P73^T can use many sugars, including D-cellobiose, D-fructose, D-trehalose, L-rhamnose, maltose, sucrose, turanose, and α -D-glucose²³. Genes that encode the enzymes required for all the steps in the glycolysis/gluconeogenesis pathways were present, except for glucose-6-phosphatase (EC:3.1.3.9), which converts D-glucose 6-phosphate to D-glucose in the gluconeogenesis pathway. In addition, strain P73^T harbors genes that encode all the enzymes needed in the pentose phosphate (PP) pathway, the Entner–Doudoroff (ED) pathway, and the tricarboxylic acid (TCA) cycle.

The principal fatty acids of strain P73^T were found to be the C18 unsaturated fatty acids²³, which are classified as long-chain fatty

acids. Unsaturated fatty acids contribute to the fluidization of membranes for adaption to low temperatures or starvation in the deep sea, and to poor aqueous solubility of aromatic hydrocarbon substrates^{23,30}. Fifty-three genes in fatty acid biosynthesis and metabolism pathways were identified, including two fatty acid desaturases (P73_2794 and P73_2801). In addition, two *fadL* long-chain fatty acid transport protein genes (P73_0184 and P73_2224) and six genes encoding the proposed fatty acid transporter (FAT) family (TC:4.C.1) of proteins were detected in the P73^T genome.

A total of 848 transport protein genes (see Supplementary Text S4 and Supplementary Data S4 for details) belonging to 102 transporter families were identified in the Transporter Classification (TC) Database (<http://tcdb.org/>)³¹. These transport protein genes made up about 17.57% of the total CDSs in the P73^T genome compared with 13.01% in the average bacterial genome in the IMG database. Many transporter genes in the P73^T genome were found to encode proteins belonging to the ATP-binding cassette (ABC) superfamily (TC:3.A.1, 371 genes)^{32,33}, the tripartite ATP-independent periplasmic transporter (TRAP-T) family (TC:2.A.56, 96 genes)³⁴, the major facilitator superfamily (MFS, TC:2.A.1, 25 genes)³⁵, the tricarboxylate transporter (TTT) family (TC:2.A.80, 8 genes)³⁶, the outer membrane protein (FadL) family (TC:1.B.9, P73_0184 and P73_2224)³⁷, and the benzoate:H⁺ symporter (BenE) family (TC:2.A.46, P73_3226)³⁵, all of which have been reported to be involved in the uptake of various aromatic compounds.

The COG analysis identified 305 genes in the P73^T genome that were assigned to the transcription (K, 7.09%) category (see Supplementary Text S5 and Supplementary Data S5 for details). Many transcriptional regulator genes in the P73^T genome were predicted to belong to the LysR-type transcriptional regulator (LTTR) family (COG0583, 53 genes)^{38,39}, the multiple antibiotic resistance regulator (MarR) family (COG1846, 19 genes)³⁹, the isocitrate lyase regulator (IcLR) family⁴⁰, the AraC, GntR, TetR, and FNR families or to two component regulatory systems, all of which have been reported to be associated with the degradation pathways of aromatic compounds³⁹.

Plasmids. Together, the five plasmids in strain P73^T contained 438 CDSs, accounting for 9.07% of the total CDSs in the genome. The COG analysis showed that the genes in four COG functional groups (information storage and processing, cellular processes and signaling, metabolism, and poorly characterized) were distributed quite differently among the plasmids, indicating a specialized function for each plasmid (see Supplementary Text S6 and Supplementary Figure S2 for details).

Phylogenetic analysis of the plasmid partition protein (*parA*) and plasmid replication protein (*rep*) genes has been used previously to gain insight into the origin and evolution of plasmids^{28,41}. Neighbor-joining phylogenetic trees were constructed with the Rep (Figure 2A) and ParA (Figure 2B) protein sequences encoded by genes from the P73^T chromosome and plasmids (see Supplementary Text S6 for details). The ParA and Rep proteins encoded from the different plasmids belonged to different clades, suggesting that divergent evolution of the *parA* and *rep* genes had occurred, and confirming the important role of gene horizontal transfer, which has been reported previously⁴¹. Based on the HTG analysis, the replicative genes P73_4797 and P73_4817 were predicted to originate from *Acetobacter aceti* ATCC 23746 (IMG Gene ID:2516943643) and the plasmid pYAN-1 of *Sphingobium yanoikuyae* ATCC 51230 (JCM 7371), respectively (Supplementary Data S3), in agreement with their predicted phylogenetic positions (Figure 2A).

Genomic comparisons with closely related bacteria. *C. indicus* P73^T in the family *Rhodobacteraceae*, was found to be closely related to species in the genera *Celeribacter*, *Pseudoruegeria*, *Lutimaribacter*, *Charonomicrobium*, and *Roseibacterium* based on similarities in the 16S rRNA gene sequences²³. All the predicted

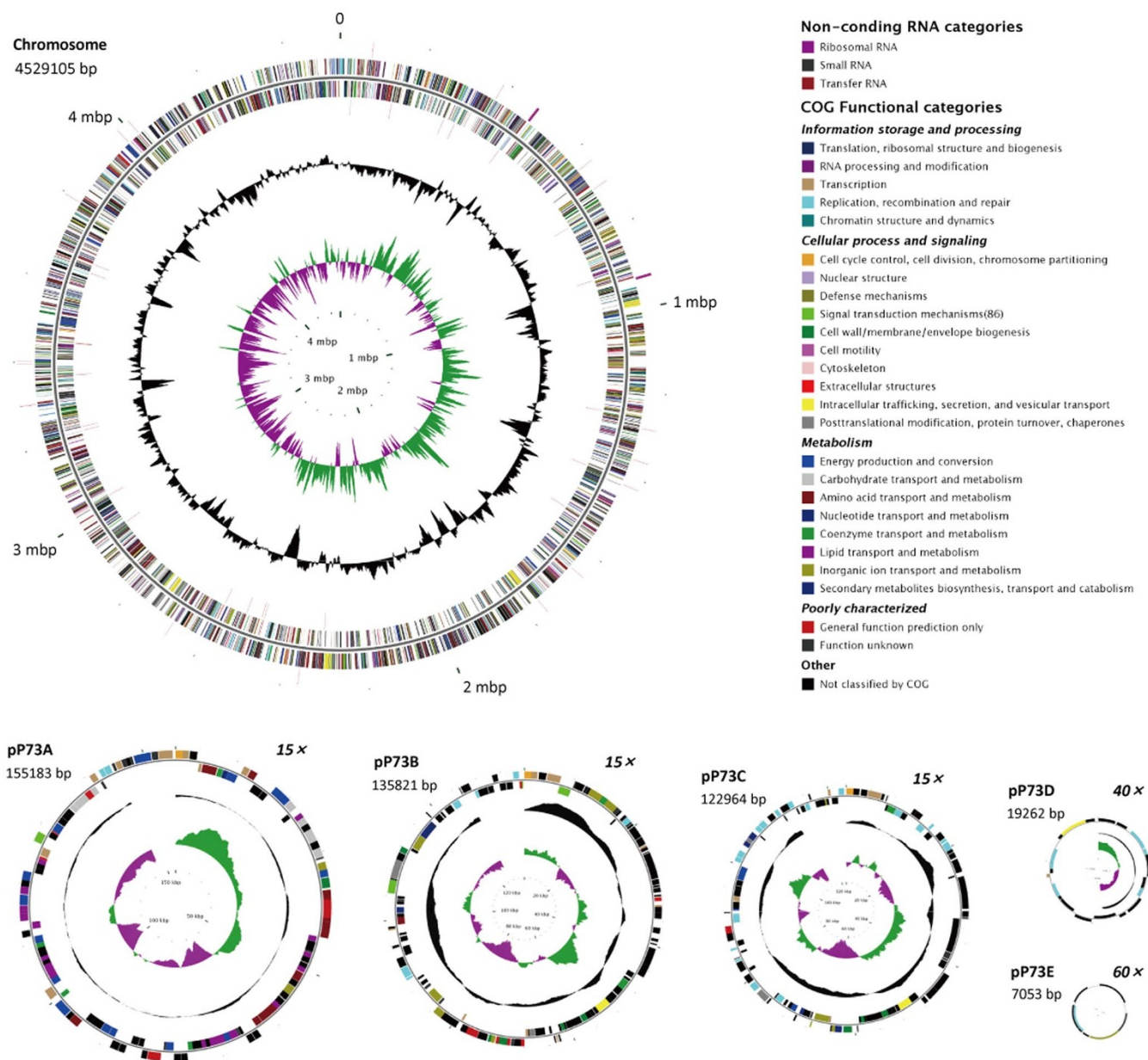


Figure 1 | Circular maps of the chromosome and five plasmids of *Celeribacter indicus* P73^T. The chromosome (4,529,105 bp) scale is in megabases beginning from the start of the *dnaA* gene. Plasmids pP73A (155,183 bp), pP73B (135,821 bp), and pP73C (122,964 bp) are shown at 15× scale relative to the chromosome scale; pP73D (19,262 bp) is shown at 40× scale; and pP73E (7,053 bp) is shown at 60× scale. Rings 1 and 4 (from the outside inwards) show the forward and reverse noncoding RNAs (tRNA, rRNA, and sRNA). Rings 2 and 3 indicate all the genes in the forward and reverse strands, respectively, and the colors indicate the predicted COG categories of the genes, as shown in the figure. Ring 5 (black) represent the G + C content (higher values outward), and ring 6 shows the G + C skew $[(G - C)/(G + C)]$, where green indicates values > 0, and purple indicates values < 0].

proteins from strain P73^T were compared against the NCBI non-redundant protein sequence database (nr, 29 May 2013) to estimate the taxonomic distribution of the proteome. The results showed that most of the proteins encoded by the chromosomal genes of strain P73^T were closely related to proteins from species in genera *Celeribacter* (2096, 47.76%), *Paracoccus* (133, 3.03%), *Oceanicola* (123, 2.80%), *Rhizobium* (122, 2.78%), *Citricella* (114, 2.60%), and *Rhodobacter* (106, 2.42%) (Figure 3), and the greatest overlap was between the proteomes of strain P73^T and *Celeribacter baekdonensis* B30. The MUMmer alignments⁴² of the strain P73^T genome with the whole genome sequences of other closely related bacteria also showed that P73^T was closest to *C. baekdonensis* B30, although the genomes of these two strains revealed extensive chromosomal rearrangements (Supplementary Figure S3). However, the

taxonomic distributions of the five plasmid proteomes of strain P73^T were different from that of the chromosome, suggesting the chromosome and the plasmids may have had potentially different origins. The major proteins of pP73A closely matched proteins in genera *Chelativorans* (18, 13.33%) and *Celeribacter* (15, 11.11%); for pP73B they matched *Roseovarius* (41, 28.67%) and *Celeribacter* (23, 16.08%); for pP73C, they matched *Celeribacter* (32, 25%) and *Maritimibacter* (25, 19.53%); for pP73D, they matched *Oceanicola* (4, 19.05%); and for pP73E, they matched *Sulfitobacter* (3, 27.27%).

Bioavailability of PAHs. Aromatic compounds, especially PAHs, are hydrophobic and insoluble in water. Biosurfactants, including glycolipids, lipopeptides and lipoproteins, phospholipids, and fatty

Table 1 | General features of the complete genome sequence of *C. indicus* P73^T

Content	Chromosome	Plasmids				
		pP73A	pP73B	pP73C	pP73D	pP73E
Size (bp)	4529105	155183	135821	122964	19262	7053
G + C content (mol%)	66.01	68.13	60.54	59.98	59.12	59.66
CDS ^a number	4389	135	143	128	21	11
Average CDS size (bp)	914	1063	739	813	792	640
Coding density (%)	88.35	92.37	84.46	84.15	85.63	82.60
CDSs assigned to COG ^b (%)	3599	134	85	77	10	3
tRNA	48	0	0	0	0	0
rRNA operon (23S, 16S and 5S)	2	0	0	0	0	0
sRNA	2	0	0	0	0	0
GenBank accession	CP004393	CP004394	CP004395	CP004396	CP004397	CP004398

^aCDS, protein-coding sequence.

^bCOG, clusters of orthologous groups.

acids, can emulsify and solubilize hydrocarbons to promote the bioavailability of substrates⁴³. Previous studies have shown that strain P73^T contained glycolipids, two phospholipids, phosphatidylglycerol, aminolipid, and one unknown lipid²³. Some genes associated with the synthesis of lipids were found in the P73^T genome: for example, 1-acylglycerol-3-phosphate *O*-acyltransferase gene *plsC* (P73_2315 and P73_4246); phosphatidate cytidyltransferase gene *cdsA* (P73_2618); CDP-diacylglycerol glycerol-3-phosphate 3-phosphatidyltransferase gene *pgsA* (P73_4294); glycerol-3-phosphate acyltransferase gene *plsX* (P73_2678); and glycerol-3-phosphate acyltransferase gene *plsY* (P73_4283)⁴⁴. Other genes involved in lipid transport and metabolism were identified based on the COG analysis (Supplementary Data S6).

Chemotaxis and cell motility can actively increase the bioavailability of PAHs^{45,46}. Many genes for flagella assembly, cell motility, and chemotaxis were identified based on the GOG and 'KEGG Orthology (KO) terms' analyses available on the IMG server⁴²; they included genes predicted to encode flagellin, flagellar motor protein, and the chemotaxis complex proteins CheY, CheD, CheR, CheW, CheA, CheB, McpH, and McpA (Supplementary Data S7). However, as reported previously, strain P73^T was non-motile and no flagella were observed²³. Flagellum assembly is a complex process in which many genes are known to be involved⁴⁷. Compared with a motile bacterium *Alteromonas taeanensis* SN2²⁷, P73^T lacked genes that encode the flagellar proteins FliO, FliJ, FlgM, FliD, and FliS. As reported previously, both FliD and FliS are essential elements in the assembly of functional flagella^{47,48}; FlgM and FliA are part of a complex regulatory network that controls flagellum number⁴⁹; and FliO, FliJ, and FlhA play roles in the energy coupling mechanism for bacterial flagellar protein export⁵⁰.

Degradation of PAHs. P73^T is capable of degrading a wide range of aromatic compounds including PAHs²³. A total of 138 genes in the P73^T genome were predicted to be involved in the metabolism of aromatic hydrocarbons. Most of the predicted catabolic genes were located in four regions of the genome: region A, position 168707–176856 bp (P73_0169–P73_0177, 8150 bp); region B, position 331325–381010 bp (P73_0326–P73_0372, 49686 bp); region C, position 828348–837837 bp (P73_0835–P73_0846, 9490 bp); and region D, position 2990411–2998597 bp (P73_2960–P73_2968, 8187 bp) (Supplementary Data S8). Other genes involved in the metabolism of aromatic hydrocarbons were found dispersed all over the genome.

Within the 49.7-kb region B, genes that were involved in the peripheral pathway for PAH degradation were identified (Figure 4). P73_0346 (biphenyl 2,3-dioxygenase subunit alpha), P73_0347 (biphenyl 2,3-dioxygenase subunit beta), P73_0348 (dioxygenase ferredoxin subunit), and P73_0354 (ferredoxin-NAD⁺ reductase) were

predicted to encode the three components of an aromatic-ring-hydroxylating dioxygenase. Downstream genes P73_0349 (2,3-dihydroxy-2,3-dihydrophenylpropionate dehydrogenase), P73_0353 (catechol 2,3-dioxygenase), P73_0352 (2-hydroxychromene-2-carboxylate isomerase), P73_0351 (*trans*-*o*-hydroxybenzylidenepyruvate hydratase-aldolase), and P73_0350 (dehydrogenase PhnF), were proposed to be responsible for the next several steps of PAH ring-hydroxylation (Figure 5). Another downstream gene P73_0355, encoding an *OmpW* family protein (COG3047), which was reported to be a receptor of colicin S4⁵¹, may play a role in the sensing of aromatic compounds. Genes P73_0329 (gentisate 1,2-dioxygenase), P73_0331 (maleylacetoacetate isomerase), and P73_0330 (fumarylpyruvate hydrolase) involved in the homogentisate ring-cleavage pathway were also found in region B (Figure 5, homogentisate pathway).

Two tRNA genes (tRNA-Lys and tRNA-Arg), suggested to be common sites for the integration of foreign sequences⁵², were found flanking each end of region B, and several putative transposases and integrases were encoded adjacent to the two tRNA genes. Several horizontally transferred genes (P73_0329–0341) likely involved in PAHs degradation were identified within region B (Supplementary Data S3). These observations suggested that the P73^T genome might have gained region B, which contained the PAH-degrading genes, via lateral gene transfer.

Based on the sequence similarities among dioxygenase alpha subunit genes, two related PAH-degrading gene clusters from *P. naphthalenivorans* CJ2²⁸ and *Polymorphum gilvum* SL003B-26A1⁴⁶ were selected for comparison with the related cluster from the genome of strain P73^T. The organization of gene clusters involved in PAHs catabolism of strains P73^T and SL003B-26A1 were almost identical, with only a minor gene rearrangement, while extensive rearrangements were found in the corresponding gene clusters in strains P73^T and CJ2, with the absence of the dehydrogenase PhnF, *trans*-*o*-hydroxybenzylidenepyruvate hydratase-aldolase, and 2-hydroxychromene-2-carboxylate isomerase genes in the gene cluster from strain CJ2.

Phthalate has been reported as a common metabolic intermediate during PAH metabolism². Region D contained genes predicted to be related to phthalate degradation (Figure 5), including P73_2964 (4,5-dihydroxyphthalate decarboxylase), P73_2965 (oxidoreductase domain-containing protein), P73_2966 (ferredoxin), and P73_2968 (phthalate 4,5-dioxygenase), which convert phthalate to another central metabolite, protocatechuate. The gene cluster for protocatechuate degradation via the β -ketoacid pathway was located in region C with a 4-hydroxybenzoate 3-monooxygenase gene, which transforms 4-hydroxybenzoate to protocatechuate, included in the cluster (Figure 5). Three sets of genes involved in the gentisate ring-cleavage pathway were found in the P73^T genome (Figure 5):

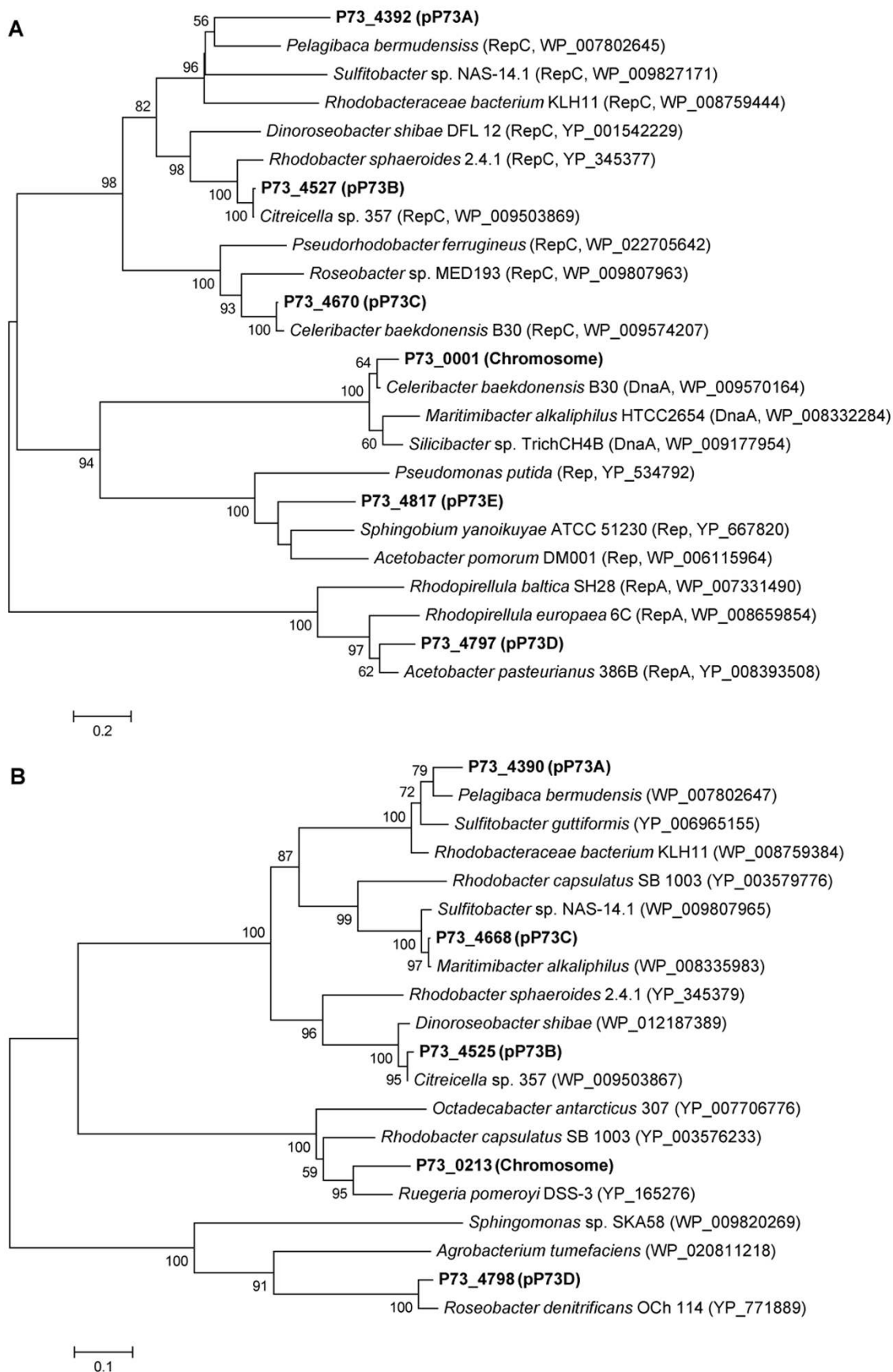


Figure 2 | Neighbor-joining phylogenetic trees constructed with replication protein (Rep) (A) and partition protein (ParA) (B) sequences from strain P73^T chromosome and plasmids. Bootstrap values > 50% (expressed as percentages of 1000 replications) are shown at branch points.

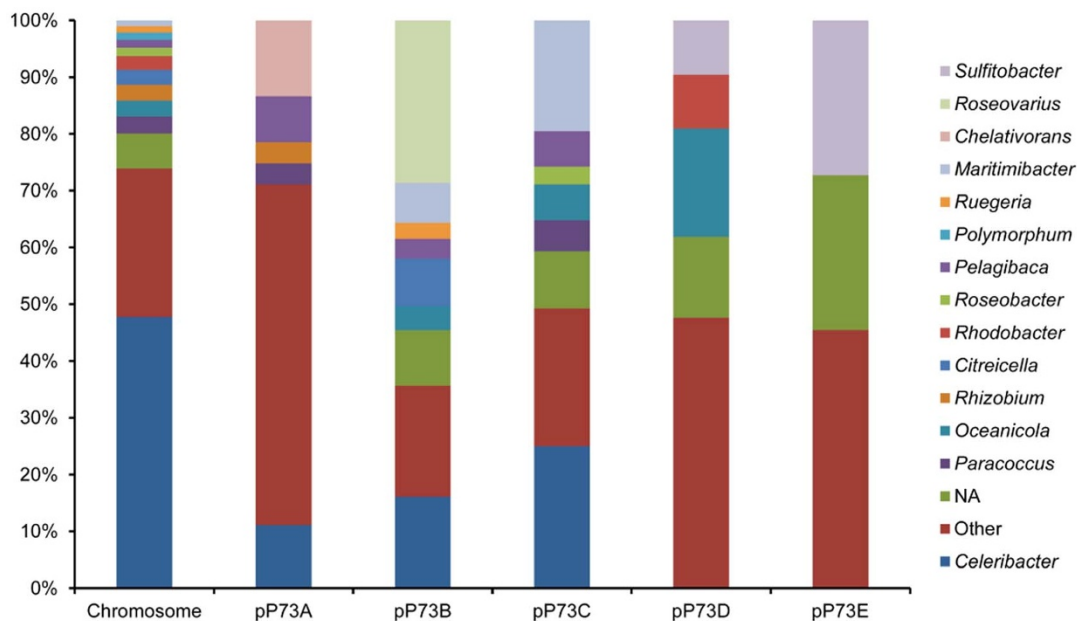


Figure 3 | Taxonomic distribution of the *C. indicus* P73^T proteome in the chromosome and plasmids. NA indicates the proteins without matches in the nr database.

P73_0175 (gentisate 1,2-dioxygenase), P73_0176 (maleylacetoacetate isomerase), and P73_0177 (fumarylpyruvate hydrolase) in region A; P73_1454 (gentisate 1,2-dioxygenase), P73_1455 (maleylacetoacetate isomerase), and P73_1456 (fumarylpyruvate hydrolase) adjacent to a salicylate hydroxylase gene (P73_1457) in the chromosome; and, P73_4775 (gentisate 1,2-dioxygenase), P73_4774 (maleylacetoacetate isomerase), and P73_4773 (fumarylpyruvate hydrolase) in plasmid pP73C.

Many other genes were predicted to encode other enzymes including aromatic-ring-hydroxylating dioxygenase, ferredoxin reductase, ferredoxin, hydroxylase, decarboxylase, cytochrome P450, monooxygenase, dehydrogenase, hydratase, thiolase, and racemase (Supplementary Data S8). These genes, often clustered with other catabolic genes or were distributed all over the genome, may also enhance the catabolic ability of strain P73^T.

Several transporter genes were found in the vicinity of aromatic catabolic genes. For instance, within region B, transporter genes P73_0342, P73_0343, and P73_0344 were adjacent to ring-hydroxylating dioxygenase genes (P73_0346 and P73_0347). P73_2224 was predicted to encode an aromatic hydrocarbon degradation membrane protein belonging to the outer membrane transport protein (OMPP1/FadL/TodX) family⁵³, and two transmembrane protein genes (P73_2223 and P73_2225) were located flanking P73_2224. In region D, an EamA-like transporter gene (P73_2962), which belonged to the drug/metabolite transporter family, was found adjacent to the phthalate degradative genes. P73_3226 encoded a benzoate membrane transport protein (BenE), which may transport benzoate-like aromatic compounds.

At the regulation level, several LTTR family transcriptional regulators were found adjacent to aromatic catabolic genes in the gen-

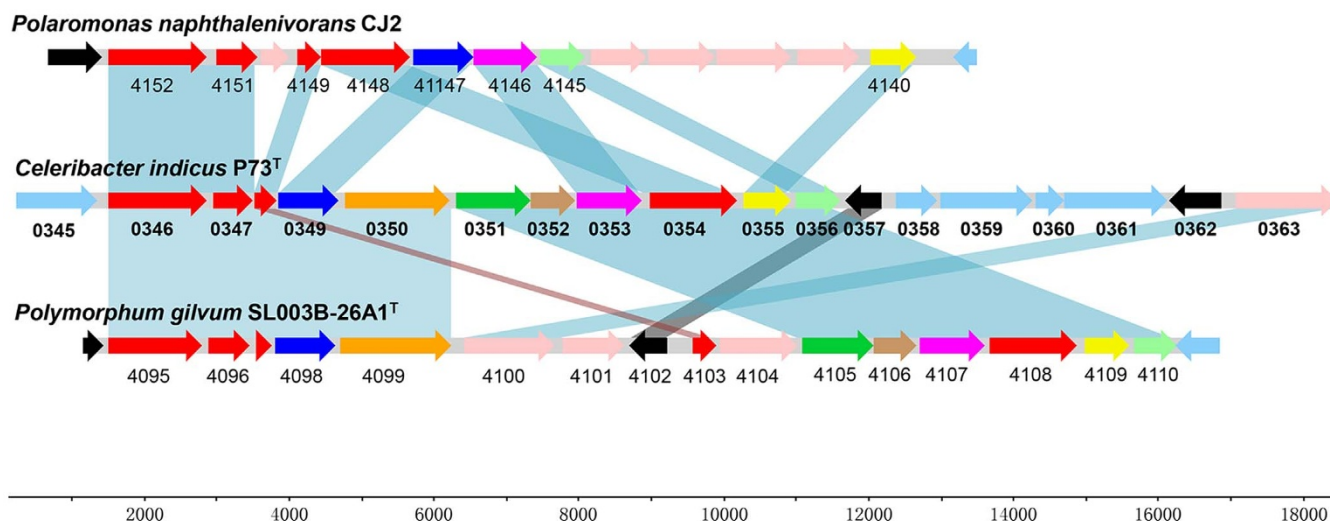


Figure 4 | Organization of the gene cluster involved in PAHs catabolism in the P73^T genome. For comparison, orthologous genes from *Polaromonas naphthalenivorans* CJ2 and *Polymorphum gilvum* SL003B-26A1 are aligned to the corresponding genes from P73^T. Orthologous genes are connected by shaded boxes. Annotation data for genes P73_0346–0357 from strain P73^T are provided in (Supplementary Data S9). The CJ2 genes Pnap_4140–4152 are located at positions 15183–26352 bp in the genome. The SL003B-26A1 genes SL003B_4095–4110 are located at positions 4401320–4416076 bp in the genome.

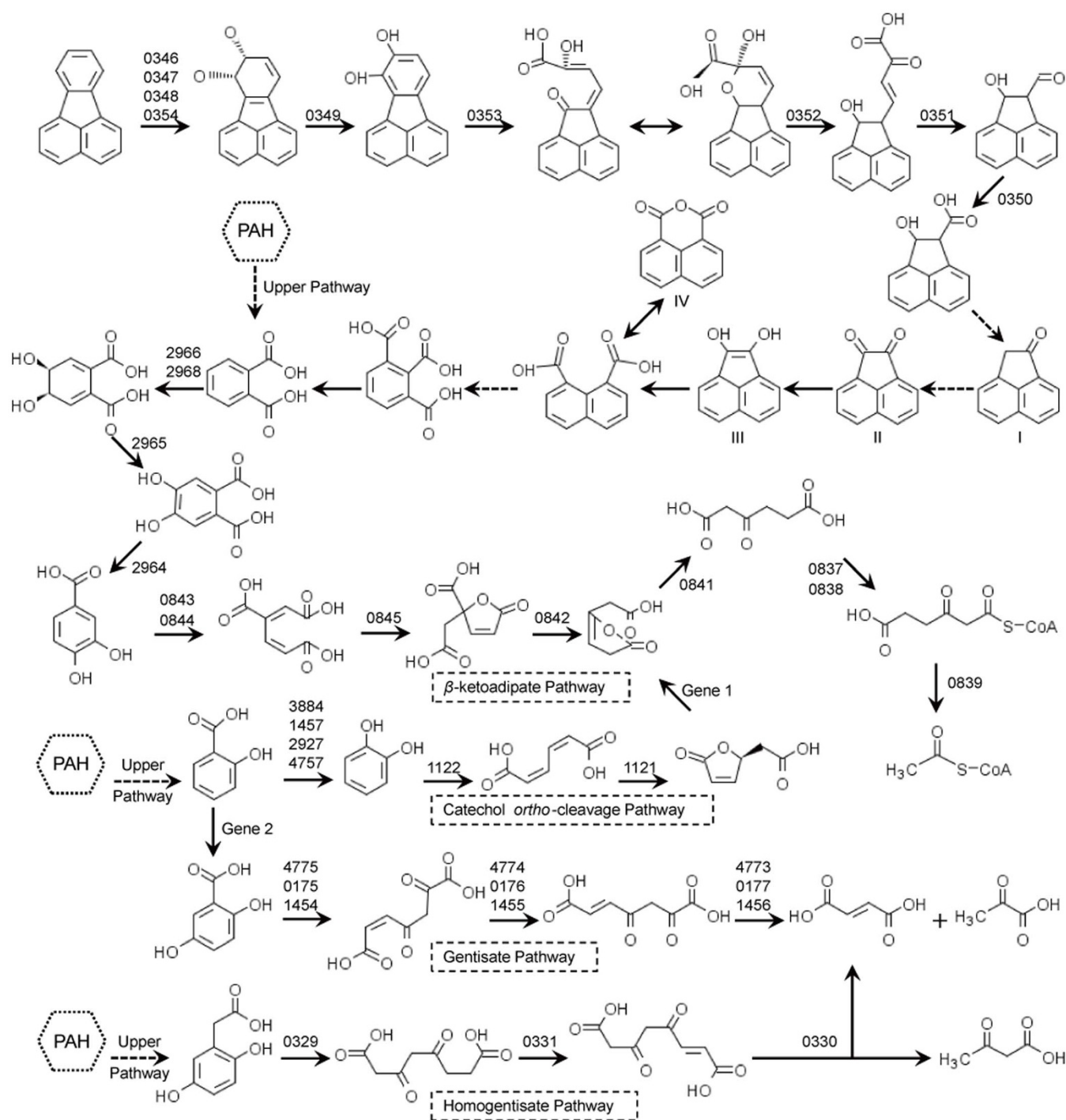


Figure 5 | Proposed pathways for the degradation of PAHs in strain P73^T. I to IV indicate the metabolites detected from the fluoranthene degradation experiment. Dashed arrows indicate two or more successive reactions. The numbers above the arrows represent the gene loci in the P73^T genome (Supplementary Data S8). No closely related homologues were found for Gene 1 (muconolactone delta-isomerase) and Gene 2 (salicylate 5-hydroxylase) in the genome.

ome, including P73_0332 regulating the homogentisate catabolic genes, P73_0840 regulating the β -ketoadipate pathway for protocatechuate degradation, and P73_1052 regulating the aromatic-ring-hydroxylating dioxygenase gene (P73_1053). In addition, three MarR family transcriptional regulator genes (P73_0337, P73_0357, and P73_2961) were predicted to be involved in aromatic compounds degradation, and P73_0836 was predicted to encode the β -ketoadipate pathway transcription regulator (PcaR), which regulates the β -ketoadipate pathway for protocatechuate degradation³⁹.

Gene knockout. P73_0346, which was located in the PAH-degrading gene cluster, was predicted to encode the aromatic-ring-hydroxylating dioxygenase alpha subunit. When this gene was disrupted by deletion with a *kan* cassette inserted, we found that the resulting mutant Δ P73_0346::*kan* was unable to use fluoranthene and naphthalene, or was defective in degrading biphenyl, phenanthrene and dibenzothiophene. These results demonstrated that P73_0346 encoded the dioxygenase subunit alpha responsible for the dioxygenation of fluoranthene, naphthalene, biphenyl, phenanthrene, and dibenzothiophene (Figure 5).



Dioxygenases. The metabolism of PAHs begins with ring hydroxylation, which is the most difficult catalytic step and usually catalyzed by ring-hydroxylating dioxygenases (RHDs). RHD is a multicomponent enzyme system that consists of a terminal oxygenase(s) and an electron transfer component(s)²⁵. Multiple paralogs to ring-hydroxylating dioxygenase subunit alpha (P73_0346, P73_1053, P73_2151, P73_2875, P73_2968, and P73_4415), ring-hydroxylating dioxygenase subunit beta (P73_0347 and P73_2150), ferredoxin (P73_0348, P73_1051, P73_2167, P73_2169, P73_2960, P73_3499, and P73_4762), and ferredoxin reductase (P73_0335, P73_0354, P73_0554, P73_1054, P73_2874, P73_4416, and P73_4758) were found in the P73^T genome. Because RHD subunit alpha plays a major role in determining substrate specificity, RHD alpha subunit has been used in phylogenetic analysis to classify RHDs⁵⁴. The phylogenetic tree of RHD alpha subunits from P73^T and other representative species is shown in Figure 6. The toluene/biphenyl family (group IV) comprises three-component enzymes from pathways for the degradation of chlorobenzenes, alkylbenzenes, benzene, and biphenyl⁵⁴. P73_0346, which could catalyze the dioxygenation of fluoranthene, naphthalene, biphenyl, phenanthrene, and dibenzothiophene, also clustered with group IV. P73_2151 may catalyze the dihydroxylation or deamination of aniline, because it was grouped with the benzoate dioxygenase family (group II), which has been reported previously to perform similar functions⁵⁴. P73_1053, P73_2875, and P73_2968, which comprised two components (an α_n oxygenase component and a reductase component), fell into the phthalate (α_n) family (group I) and were predicted to be involved in the degradation of aromatic compounds structurally similar to phthalate. The protein encoded by the plasmid gene P73_4415 clustered with some phenylpropionate dioxygenases, which may form a new family (group VII). No closely related homologues were found in the P73^T genome for the naphthalene family (group III), the Gram⁺ PAH/phthalate family (group V), or the salicylate dioxygenases family (group VI).

Several dioxygenases that can transform fluoranthene have been reported previously. For example, ArhA1 [GenBank:BAD34447] from *Sphingomonas* sp. A4⁵⁵, PhnA1a [GenBank:CAG17576] from *Sphingomonas* sp. CHY-1⁵⁶, and PhnA1f [GenBank:ABW37061] from *Sphingomonas* sp. LH128⁵⁷, all of which belong to the naphthalene family (group III), can convert fluoranthene to the corresponding dihydrodiol or monohydroxylated products. NidA3 [GenBank:ABM11369] from *Mycobacterium vanbaalenii* PYR-1², and PhdA [GenBank:ABK27720] from *Mycobacterium* sp. SNP11⁵⁸, which were clustered with Gram⁺ PAH/phthalate family (group V) dioxygenases, can oxidize fluoranthene. Fluoranthene 2,3-dioxygenase CarAa [GenBank:BAA21728] from *Pseudomonas* sp. CA10⁵⁹ was grouped with the phthalate (α_n) family (group I), while Mvan_0533 [GenBank:ABM11377] and Mvan_0539 [GenBank:ABM11383] from *Mycobacterium vanbaalenii* PYR-1², FlnA1 [GenBank:ABV68886] from *Sphingomonas* sp. LB126⁶⁰, and IdoA [GenBank:AF474963] from *Pseudomonas alcaligenes* PA-10⁶¹, all of which were also reported to oxidize fluoranthene, did not fall into any dioxygenase family group. To our knowledge, P73_0346 is the first fluoranthene dioxygenase to be identified within the RHD alpha subunit toluene/biphenyl family (group IV).

Ring-cleaving dioxygenases catalyze critical dearomatization steps in the PAH degradation pathway²⁵. Nine genes in the genome of P73^T were predicted to encode different ring-cleaving dioxygenases, namely, gentisate 1,2-dioxygenase (P73_0175, P73_1454, and P73_4775), homogentisate 1,2-dioxygenase (P73_0329), catechol 2,3-dioxygenase (P73_0353), extradiol ring-cleavage dioxygenase III subunit B (P73_0507), protocatechuate 3,4-dioxygenase (P73_0843 and P73_0844), and catechol 1,2-dioxygenase (P73_1122).

Fluoranthene degradation. It has been reported previously that strain P73^T can degrade fluoranthene, a high-molecular-weight

PAH that has been used as a model PAH for biodegradation studies. Growing strain P73^T with fluoranthene resulted in the accumulation of a brown compound that had a maximal absorbance at 225 nm. Four major metabolites were confirmed during fluoranthene degradation using gas chromatography-mass spectrometry (GC-MS): acenaphthylene-1(2H)-one (I), acenaphthenequinone (II), 1,2-dihydroxyacenaphthylene (III) and 1,8-naphthalic anhydride (IV) (Supplementary Figures S4–S7), indicating that strain P73^T metabolized fluoranthene through the C-7,8 dioxygenation pathway. Indeed, it has been suggested previously that 1,8-naphthalic anhydride (IV) is formed by the thermal decomposition of naphthalene-1,8-dicarboxylic acid⁴.

The C-7,8 dioxygenation pathway for fluoranthene degradation was proposed initially in *Alcaligenes denitrificans* WW1²⁴, *Mycobacterium vanbaalenii* PYR-1⁴, and *Mycobacterium* sp. AP1¹⁸. Based on the genomic analysis and the metabolic data in this study, and on studies reported previously^{2,4,5,18}, here we propose metabolic pathways for fluoranthene and assign the most probable genes to each enzymatic reaction in the pathways (Figure 5). Firstly, fluoranthene is dioxygenated at the C-7,8 positions to form fluoranthene *cis*-7,8-dihydrodiol, which is then catalyzed by an RHD encoded by P73_0346, P73_0347, P73_0348, and P73_0354. The resultant fluoranthene *cis*-7,8-dihydrodiol is then dehydrogenated by dihydrodiol dehydrogenase (P73_0349) to produce 7,8-dihydroxyfluoranthene, which is subjected to extradiol ring rupture by an extradiol-type ring-cleavage dioxygenase (P73_0353) to form (2Z,4Z)-2-hydroxy-4-(2-oxoacenaphthylene-1(2H)-ylidene)but-2-enoic acid⁴. Subsequently, a ketal bond is formed automatically and the resulted *cis* isomer is transformed to (*E*)-4-(2-hydroxy-1,2-dihydroacenaphthylene-1-yl)-2-oxobut-3-enoic acid by an isomerase (P73_0352)⁶². The next step is catalyzed by hydratase-aldolase (P73_0351), which releases a pyruvate to produce 2-hydroxy-1,2-dihydroacenaphthylene-1-carbaldehyde, the aldehyde group of which is then oxidized to a carboxyl group⁶³. Next, acenaphthylene-1(2H)-one (I) and acenaphthenequinone (II) are formed through two or more successive reactions. Acenaphthenequinone (II) can be reduced to 1,2-dihydroxyacenaphthylene (III), after which the central metabolite naphthalene-1,8-dicarboxylic acid, which can be decomposed thermally to 1,8-naphthalic anhydride (IV), is formed⁴. Further mineralization produces 1,2,3-benzenetricarboxylic acid, phthalate, and protocatechuate, which are then metabolized through the β -ketoadipate pathway mentioned above (Figure 5).

The gentisate ring-cleavage pathway⁶⁴, catechol *ortho* ring-cleavage pathway⁶⁵, and homogentisate ring-cleavage pathway⁶⁶ have also been reported to be involved in the central pathways for PAHs shown in Figure 5. All the genes involved in these central pathways were found in the genome of P73^T, except for genes that encode muconolactone D-isomerase (Figure 5, Gene 1) and salicylate 5-hydroxylase (Figure 5, Gene 2).

Comparison of strain P73^T with *Celeribacter baekdonensis* B30. Strain B30 was isolated from deep-sea sediment of the Arctic Ocean (W170°29.31', N87°04.27') at a water depth of 4000 m by our group. It was named *Celeribacter baekdonensis* based on the 16S rRNA gene sequence, which shared 99.79% similarity with that of *Celeribacter baekdonensis* L-6⁷⁶⁷. The draft B30 genome sequence is available in GenBank (Accession: AMRK00000000). The PAH degradation test showed that strain B30 was unable to degrade naphthalene, phenanthrene, pyrene, or fluoranthene (unpublished observations).

Based on the COG analysis of the two *Celeribacter* genomes, we found that compared with strain B30, genes involved in amino acid transport and metabolism (E, 10.34%) were less abundant in strain P73^T, while genes involved in inorganic ion transport and metabolism (P, 9.19%), and replication, recombination and repair (L, 6.42%) (12.53%, 6.31% and 4.06%, respectively) were more abundant. The abundances of genes in others COGs were similar in the two strains.

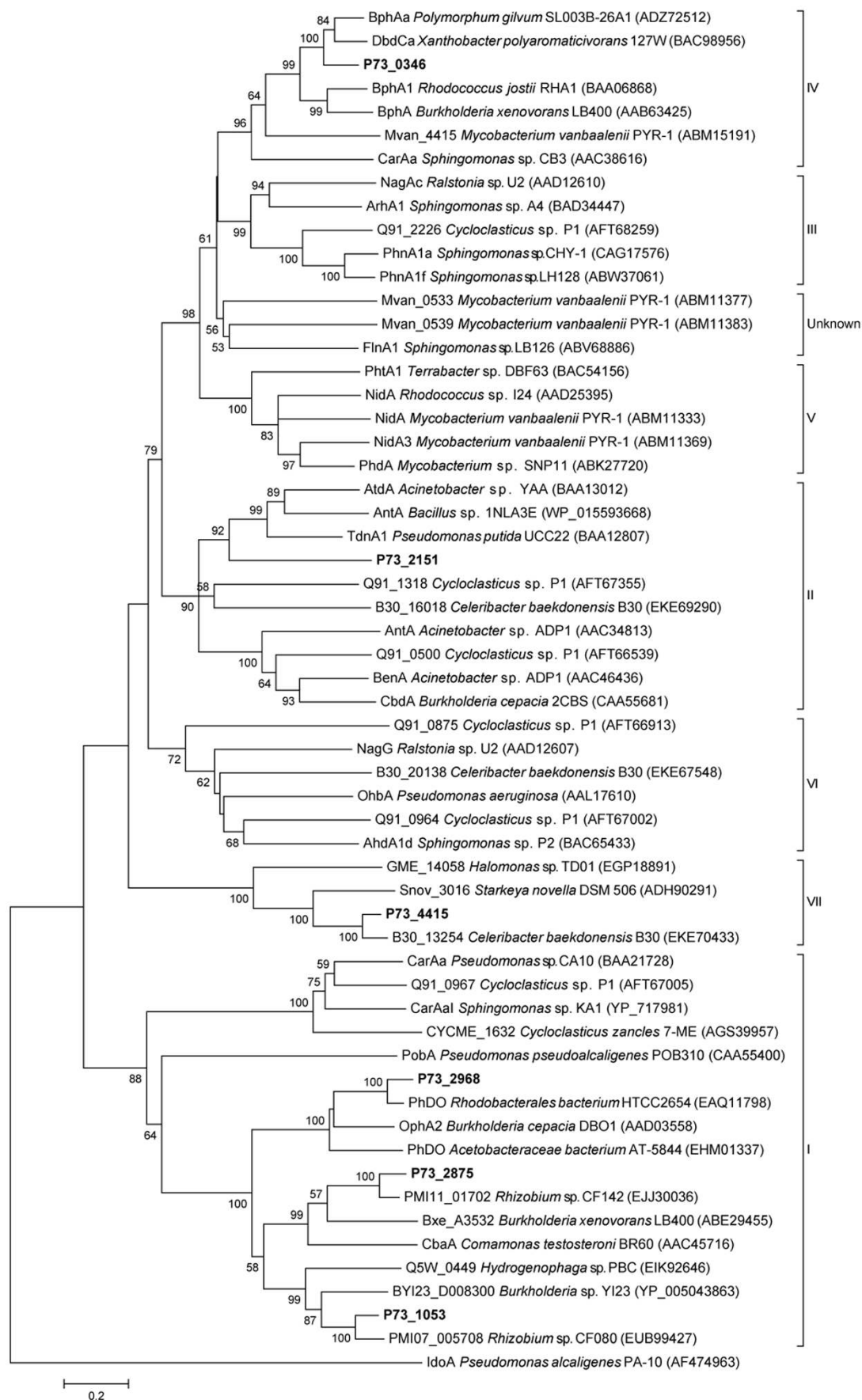


Figure 6 | Phylogenetic tree constructed using the sequences of alpha subunits of aromatic ring hydroxylating dioxygenases. The P73^T proteins are shown in bold. Bootstrap values > 50% (expressed as the percentages of 1000 replications) are shown at the branch points.



The IMG ‘Phylogenetic Profiler for Single Genes’ was used to find genes in the P73^T genome that had no homologs in the B30 genome. A total of 1484 genes in P73^T with no homologs in B30 were detected (Supplementary Data S9). Interestingly, almost all the genes in regions B and D of the P73^T genome—which are responsible for PAH degradation, especially the metabolism of fluoranthene—were absent in the B30 genome. Only three RHDs were identified in the B30 genome; their phylogenetic positions are shown in Figure 5. The B30 genome had no homologues for the dioxygenases encoded by P73_0346, P73_0153, P73_2875, and P73_2968, which were predicted to be involved in the metabolism of PAHs in strain P73^T.

Discussion

Our analyses of the complete genome of *C. indicus* P73^T have expanded the knowledge of the mechanisms used to metabolize PAHs in this bacterium. The P73^T genome contains 138 candidate genes that may be involved in the metabolism of aromatic compounds, including genes that encode six ring hydroxylating dioxygenases, eight ring cleaving dioxygenases, other catabolic enzymes, transcriptional regulators, and transporters in the degradation pathways. We found that genetic acquisitions via lateral gene transfer may have contributed to the ability of strain P73^T to catabolize aromatic compounds. Notably, region B of the genome, which contained the PAH-degrading genes and were absent in another bacterium of *Celeribacter*, strain B30, was predicted to have been acquired via lateral gene transfer. This study will provide a molecular basis for future research into the functions of the P73^T genes.

Aromatic ring hydroxylation is the most difficult catalytic step of fluoranthene degradation. Several dioxygenases that can transform fluoranthene have been reported previously, including ArhA1 [GenBank:BAD34447]⁵⁵, PhnA1a [GenBank:CAG17576]⁵⁶, PhnA1f [GenBank:ABW37061]⁵⁷, NidA3 [GenBank:ABM11369]², PhdA [GenBank:ABK27720]⁵⁸, CarAa [GenBank:BAA21728]⁵⁹, Mvan_0533 [GenBank:ABM11377] and Mvan_0539 [GenBank:ABM11383]², FlnA1 [GenBank:ABV68886]⁶⁰, and IdoA (GenBank:AF474963)⁶¹. However, none of these belong to the toluene/biphenyl family (group IV). The P73_0346 gene represents the first identified fluoranthene 7,8-dioxygenase and the first toluene/biphenyl family fluoranthene dioxygenase to be reported. P73_0346 is also responsible for the dioxygenation of naphthalene, biphenyl, phenanthrene and dibenzothiophene, which are structurally similar to fluoranthene.

The proposed C-7,8 dioxygenation pathway for fluoranthene metabolism in strain P73^T is consistent with the pathway that involved extradiol cleavage of 7,8-dihydroxyfluoranthene reported previously^{2,18}. However, the C-7,8 dioxygenation pathway was the only pathway detected in strain P73^T, in contrast to other bacteria, which typically have two or more different pathways for fluoranthene metabolism^{2,5,17,18}. Therefore, strain P73^T, the first fluoranthene-degrading *Rhodobacteraceae* bacterium reported, may be a useful strain in which the C-7,8 dioxygenation pathway involving extradiol cleavage of 7,8-dihydroxyfluoranthene can be studied. Further, P73^T is a novel PAH-degrading bacterium that may have the potential to be applied in marine oil spill bioremediation.

Although this study presents the genomic complement of PAH degradation and the fluoranthene degradative pathway in strain P73^T, finding out the complete physiology of the bacterium towards PAH degradation still demands more explorations. Additional experiment is necessary to study the functions of catabolic gene as well as the mechanisms of regulation and transportation in strain P73^T with respect to PAH degradation. It is also interesting to study the role of the five plasmids in the PAH metabolism.

Methods

Bacterial growth and DNA extraction. *C. indicus* P73^T, isolated from deep-sea sediment of the Indian Ocean, and *C. baekdonensis* B30, isolated from deep-sea sediment of the Arctic Ocean, were grown on 216L agar medium at 28°C²³. Genomic DNA was extracted according to the method of Ausubel *et al.*⁶⁸.

Genome sequencing and analysis. The sequencing of the P73^T and B30 genomes was carried out at the Beijing Genomics Institute (BGI; Shenzhen, China) using Solexa paired-end sequencing technology⁶⁹. Gaps between the assembled P73^T scaffolds were filled by generating PCR products and sequencing them using an ABI 3730 capillary sequencer (Applied Biosystems, Foster City, CA).

Protein coding sequences were predicted using Glimmer 3.0⁷⁰. The genomic analyses were performed as described previously⁷¹ using the tools available on the Integrated Microbial Genomes (IMG) server (<https://img.jgi.doe.gov>)⁷². Genomic islands (GIs) were analyzed using IslandViewer (<http://www.pathogenomics.sfu.ca/islandviewer>)⁷³.

Mutant generation. A gene deletion P73^T mutant was generated using of the *cre-lox* recombination method reported by Marx and Lidstrom⁷². *Escherichia coli* WM3064 was used as the conjugal donor strain, and pJK100 (allelic-exchange vector, Tc^R, Km^R) was used as the suicide vector⁷³. More information on all aspects of the mutant generation method can be found in the Supplementary Text S7.

Analysis of intermediate metabolites in fluoranthene degradation. Strain P73^T was grown in artificial sea water (ASM) medium⁷⁴ supplemented with fluoranthene (20 mg/L) as the sole source of carbon and energy at 28°C and 160 rpm. Metabolites were extracted and processed for analysis as described previously^{4,5} with slight modification (see Supplementary Text S8 for details). After silylation with *N,O*-bis(trimethylsilyl)-trifluoroacetamide with 1% trimethylchlorosilane, the samples were analyzed by GC-MS (QP2010, Shimadzu, Kyoto, Japan) in the SCAN mode. Metabolites were determined based on the molecular and fragment ions in the mass spectra and the chromatographic retention time (*R_t*) of authentic compounds.

- Kanally, R. & Harayama, S. Biodegradation of high-molecular-weight polycyclic aromatic hydrocarbons by bacteria. *J. Bacteriol.* **182**, 2059–2067 (2000).
- Kweon, O. *et al.* Polycyclic Aromatic Hydrocarbon Metabolic Network in *Mycobacterium vanbaalenii* PYR-1. *J. Bacteriol.* **193**, 4326–4337 (2011).
- Fuchs, G., Boll, M. & Heider, J. Microbial degradation of aromatic compounds - from one strategy to four. *Nat. Rev. Microbiol.* **9**, 803–816 (2011).
- Kweon, O. *et al.* A polyomic approach to elucidate the fluoranthene-degradative pathway in *Mycobacterium vanbaalenii* PYR-1. *J. Bacteriol.* **189**, 4635–4647 (2007).
- Lee, S. E., Seo, J. S., Keum, Y. S., Lee, K. J. & Li, Q. X. Fluoranthene metabolism and associated proteins in *Mycobacterium* sp. JS14. *Proteomics* **7**, 2059–2069 (2007).
- Keum, Y. S., Seo, J. S., Hu, Y. & Li, Q. X. Degradation pathways of phenanthrene by *Sinorhizobium* sp. C4. *Appl. Microbiol. Biotechnol.* **71**, 935–941 (2006).
- van Herwijnen, R. *et al.* Elucidation of the metabolic pathway of fluorene and cometabolic pathways of phenanthrene, fluoranthene, anthracene and dibenzothiophene by *Sphingomonas* sp. LB126. *Res. Microbiol.* **154**, 199–206 (2003).
- Akhtar, N., Ghauri, M. A., Anwar, M. A. & Akhtar, K. Analysis of the dibenzothiophene metabolic pathway in a newly isolated *Rhodococcus* spp. *FEMS Microbiol. Lett.* **301**, 95–102 (2009).
- Šepič, E., Brčić, M. & Leskovsek, H. Degradation of fluoranthene by *Pasteurella* sp. IFA and *Mycobacterium* sp. PYR-1: isolation and identification of metabolites. *J. Appl. Microbiol.* **85**, 746–754 (1998).
- Mallick, S., Chatterjee, S. & Dutta, T. K. A novel degradation pathway in the assimilation of phenanthrene by *Staphylococcus* sp strain PN/Y via meta-cleavage of 2-hydroxy-1-naphthoic acid: formation of *trans*-2,3-dioxo-5-(2'-hydroxyphenyl)pent-4-enoic acid. *Microbiology* **153**, 2104–2115 (2007).
- Marx, C. J., Miller, J. A., Chistoserdova, L. & Lidstrom, M. E. Multiple formaldehyde oxidation/detoxification pathways in *Burkholderia fungorum* LB400. *J. Bacteriol.* **186**, 2173–2178 (2004).
- Prabhu, Y. & Phale, P. S. Biodegradation of phenanthrene by *Pseudomonas* sp. strain PP2: novel metabolic pathway, role of biosurfactant and cell surface hydrophobicity in hydrocarbon assimilation. *Appl. Microbiol. Biotechnol.* **61**, 342–351 (2003).
- Baboshin, M. *et al.* Conversion of polycyclic aromatic hydrocarbons by *Sphingomonas* sp. VKM B-2434. *Biodegradation* **19**, 567–576 (2008).
- Weissenfels, W. D., Beyer, M. & Klein, J. Degradation of phenanthrene, fluorene and fluoranthene by pure bacterial cultures. *Appl. Microbiol. Biotechnol.* **32**, 479–484 (1990).
- Juhász, A. L., Britz, M. L. & Stanley, G. A. Degradation of fluoranthene, pyrene, benz[*a*]anthracene and dibenz[*a,h*]anthracene by *Burkholderia cepacia*. *J. Appl. Microbiol.* **83**, 189–198 (1997).
- Gordon, L. & Dobson, A. D. Fluoranthene degradation in *Pseudomonas alcaligenes* PA-10. *Biodegradation* **12**, 393–400 (2001).
- Rehmann, K., Hertkorn, N. & Ketrup, A. A. Fluoranthene metabolism in *Mycobacterium* sp. strain KR20: identity of pathway intermediates during degradation and growth. *Microbiology* **147**, 2783–2794 (2001).
- López, Z., Vila, J., Minguiñón, C. & Grifoll, M. Metabolism of fluoranthene by *Mycobacterium* sp. strain AP1. *Appl. Microbiol. Biotechnol.* **70**, 747–756 (2006).
- Walter, U., Beyer, M., Klein, J. & Rehm, H.-J. Degradation of pyrene by *Rhodococcus* sp. UW1. *Appl. Microbiol. Biotechnol.* **34**, 671–676 (1991).
- Wu, Y. R. *et al.* Isolation of marine benzo[*a*]pyrene-degrading *Ochrobactrum* sp. BAP5 and proteins characterization. *J. Environ. Sci. (China)* **21**, 1446–1451 (2009).



21. Yuan, J., Lai, Q., Zheng, T. & Shao, Z. *Novosphingobium indicum* sp. nov., a polycyclic aromatic hydrocarbon-degrading bacterium isolated from a deep-sea environment. *Int. J. Syst. Evol. Microbiol.* **59**, 2084–2088 (2009).
22. Geiselbrecht, A. D., Hedlund, B. P., Tichi, M. A. & Staley, J. T. Isolation of marine polycyclic aromatic hydrocarbon (PAH)-degrading *Cycloclasticus* strains from the Gulf of Mexico and comparison of their PAH degradation ability with that of Puget Sound *Cycloclasticus* strains. *Appl. Environ. Microbiol.* **64**, 4703–4710 (1998).
23. Lai, Q., Cao, J., Yuan, J., Li, F. & Shao, Z. *Celeribacter indicus* sp. nov. a polycyclic aromatic hydrocarbon-degrading bacterium from deep-sea sediment and reclassification of *Huaishuia halophila* as *Celeribacter halophilus* comb. nov. *Int. J. Syst. Evol. Microbiol.* **64**, 4160–4167 (2014).
24. Weissenfels, W., Beyer, M., Klein, J. & Rehm, H. Microbial metabolism of fluoranthene: isolation and identification of ring fission products. *Appl. Microbiol. Biotechnol.* **34**, 528–535 (1991).
25. Kim, S. J., Kweon, O., Jones, R. C., Edmondson, R. D. & Cerniglia, C. E. Genomic analysis of polycyclic aromatic hydrocarbon degradation in *Mycobacterium vanbaalenii* PYR-1. *Biodegradation* **19**, 859–881 (2008).
26. Hickey, W. J., Chen, S. & Zhao, J. The *phn* Island: A New Genomic Island Encoding Catabolism of Polynuclear Aromatic Hydrocarbons. *Front. Microbiol.* **3**, 125 (2012).
27. Math, R. K. *et al.* Comparative genomics reveals adaptation by *Alteromonas* sp. SN2 to marine tidal-flat conditions: cold tolerance and aromatic hydrocarbon metabolism. *PLoS ONE* **7**, e35784 (2012).
28. Yagi, J. M., Sims, D., Brettin, T., Bruce, D. & Madsen, E. L. The genome of *Polaromonas naphthalenivorans* strain CJ2, isolated from coal tar-contaminated sediment, reveals physiological and metabolic versatility and evolution through extensive horizontal gene transfer. *Environ. Microbiol.* **11**, 2253–2270 (2009).
29. Langille, M. G. & Brinkman, F. S. IslandViewer: an integrated interface for computational identification and visualization of genomic islands. *Bioinformatics* **25**, 664–665 (2009).
30. Beales, N. Adaptation of microorganisms to cold temperatures, weak acid preservatives, low pH, and osmotic stress: a review. *Compr. Rev. Food Sci. Food Saf.* **3**, 1–20 (2004).
31. Saier, M. H., Jr., Yen, M. R., Noto, K., Tamang, D. G. & Elkan, C. The Transporter Classification Database: recent advances. *Nucleic Acids Res.* **37**, D274–278 (2009).
32. Davidson, A. L., Dassa, E., Orelle, C. & Chen, J. Structure, function, and evolution of bacterial ATP-binding cassette systems. *Microbiol. Mol. Biol. Rev.* **72**, 317–364 (2008).
33. Chang, H. K., Dennis, J. J. & Zylstra, G. J. Involvement of two transport systems and a specific porin in the uptake of phthalate by *Burkholderia* spp. *J. Bacteriol.* **191**, 4671–4673 (2009).
34. Mulligan, C., Fischer, M. & Thomas, G. H. Tripartite ATP-independent periplasmic (TRAP) transporters in bacteria and archaea. *FEMS Microbiol. Rev.* **35**, 68–86 (2011).
35. Chaudhry, M. T. *et al.* Genome-wide investigation of aromatic acid transporters in *Corynebacterium glutamicum*. *Microbiology* **153**, 857–865 (2007).
36. Hosaka, M. *et al.* Novel tripartite aromatic acid transporter essential for terephthalate uptake in *Comamonas* sp. strain E6. *Appl. Environ. Microbiol.* **79**, 6148–6155 (2013).
37. Kahng, H. Y., Byrne, A. M., Olsen, R. H. & Kukor, J. J. Characterization and role of *tbuX* in utilization of toluene by *Ralstonia pickettii* PKO1. *J. Bacteriol.* **182**, 1232–1242 (2000).
38. Maddocks, S. E. & Oyston, P. C. Structure and function of the LysR-type transcriptional regulator (LTTR) family proteins. *Microbiology* **154**, 3609–3623 (2008).
39. Tropel, D. & van der Meer, J. R. Bacterial transcriptional regulators for degradation pathways of aromatic compounds. *Microbiol. Mol. Biol. Rev.* **68**, 474–500 (2004).
40. Molina-Henares, A. J., Krell, T., Eugenia Guazzaroni, M., Segura, A. & Ramos, J. L. Members of the IclR family of bacterial transcriptional regulators function as activators and/or repressors. *FEMS Microbiol. Rev.* **30**, 157–186 (2006).
41. Mazur, A., Majewska, B., Stasiak, G., Wielbo, J. & Skorupska, A. *repABC*-based replication systems of *Rhizobium leguminosarum* bv. *trifolii* TA1 plasmids: incompatibility and evolutionary analyses. *Plasmid* **66**, 53–66 (2011).
42. Markowitz, V. M. *et al.* The integrated microbial genomes system: an expanding comparative analysis resource. *Nucleic Acids Res.* **38**, D382–390 (2010).
43. Kuyukina, M. S. & Ivshina, I. B. In *Biology of Rhodococcus* Vol. 16 *Microbiology Monographs* (ed Héctor M. Alvarez) Ch. *Rhodococcus* Biosurfactants: Biosynthesis, Properties, and Potential Applications, 291–313 (Springer, 2010).
44. Himmelreich, R. *et al.* Complete sequence analysis of the genome of the bacterium *Mycoplasma pneumoniae*. *Nucleic Acids Res.* **24**, 4420–4449 (1996).
45. Velasco-Casal, P., Wick, L. Y. & Ortega-Calvo, J. J. Chemoeffectors decrease the deposition of chemotactic bacteria during transport in porous media. *Environ. Sci. Technol.* **42**, 1131–1137 (2008).
46. Nie, Y. *et al.* The genome sequence of *Polymorphum gilvum* SL003B-26A1^T reveals its genetic basis for crude oil degradation and adaptation to the saline soil. *PLoS ONE* **7**, e31261 (2012).
47. Kim, J. S., Chang, J. H., Chung, S. I. & Yum, J. S. Molecular cloning and characterization of the *Helicobacter pylori* *fljD* gene, an essential factor in flagellar structure and motility. *J. Bacteriol.* **181**, 6969–6976 (1999).
48. Mukherjee, S., Babbitzke, P. & Kearns, D. B. FliW and FliS function independently to control cytoplasmic flagellin levels in *Bacillus subtilis*. *J. Bacteriol.* **195**, 297–306 (2013).
49. Wilkinson, D. A., Chacko, S. J., Venien-Bryan, C., Wadhams, G. H. & Armitage, J. P. Regulation of flagellum number by FliA and FlgM and role in biofilm formation by *Rhodobacter sphaeroides*. *J. Bacteriol.* **193**, 4010–4014 (2011).
50. Macnab, R. M. Type III flagellar protein export and flagellar assembly. *Biochim. Biophys. Acta* **1694**, 207–217 (2004).
51. Pils, H., Smajs, D. & Braun, V. Characterization of colicin S4 and its receptor, OmpW, a minor protein of the *Escherichia coli* outer membrane. *J. Bacteriol.* **181**, 3578–3581 (1999).
52. Hacker, J., Blum-Oehler, G., Muhldorfer, I. & Tschape, H. Pathogenicity islands of virulent bacteria: structure, function and impact on microbial evolution. *Mol. Microbiol.* **23**, 1089–1097 (1997).
53. van den Berg, B., Black, P. N., Clemons, W. M., Jr. & Rapoport, T. A. Crystal structure of the long-chain fatty acid transporter FadL. *Science* **304**, 1506–1509 (2004).
54. Parales, R. E. & Resnick, S. M. Aromatic ring hydroxylating dioxygenases. *Pseudomonas* **4**, 287–340 (2006).
55. Pinyakong, O. *et al.* Isolation and characterization of genes encoding polycyclic aromatic hydrocarbon dioxygenase from acenaphthene and acenaphthylene degrading *Sphingomonas* sp. strain A4. *FEMS Microbiol. Lett.* **238**, 297–305 (2004).
56. Jouanneau, Y., Meyer, C., Jakoncic, J., Stojanoff, V. & Gaillard, J. Characterization of a naphthalene dioxygenase endowed with an exceptionally broad substrate specificity toward polycyclic aromatic hydrocarbons. *Biochemistry* **45**, 12380–12391 (2006).
57. Schuler, L. *et al.* Characterization of a ring-hydroxylating dioxygenase from phenanthrene-degrading *Sphingomonas* sp. strain LH128 able to oxidize benz[a]anthracene. *Appl. Microbiol. Biotechnol.* **83**, 465–475 (2009).
58. Pagnout, C. *et al.* Isolation and characterization of a gene cluster involved in PAH degradation in *Mycobacterium* sp. strain SNP11: Expression in *Mycobacterium smegmatis* mc²155. *Res. Microbiol.* **158**, 175–186 (2007).
59. Nojiri, H. *et al.* Diverse oxygenations catalyzed by carbazole 1,9a-dioxygenase from *Sphingomonas* sp. Strain CA10. *J. Bacteriol.* **181**, 3105–3113 (1999).
60. Schuler, L. *et al.* Characterization of a novel angular dioxygenase from fluorene-degrading *Sphingomonas* sp. strain LB126. *Appl. Environ. Microbiol.* **74**, 1050–1057 (2008).
61. Alemayehu, D., Gordon, L. M., O'Mahony, M. M., O'Leary, N. D. & Dobson, A. D. Cloning and functional analysis by gene disruption of a novel gene involved in indigo production and fluoranthene metabolism in *Pseudomonas alcaligenes* PA-10. *FEMS Microbiol. Lett.* **239**, 285–293 (2004).
62. Thompson, L. C. *et al.* 2-Hydroxychromene-2-carboxylic acid isomerase: a kappa class glutathione transferase from *Pseudomonas putida*. *Biochemistry* **46**, 6710–6722 (2007).
63. Keck, A. *et al.* Identification and functional analysis of the genes for naphthalenesulfonate catabolism by *Sphingomonas xenophaga* BN6. *Microbiology* **152**, 1929–1940 (2006).
64. Liu, T. T. *et al.* Functional characterization of a gene cluster involved in gentisate catabolism in *Rhodococcus* sp. strain NCIMB 12038. *Appl. Microbiol. Biotechnol.* **90**, 671–678 (2011).
65. Brzostowicz, P. C., Reams, A. B., Clark, T. J. & Neidle, E. L. Transcriptional cross-regulation of the catechol and protocatechuate branches of the *beta*-ketoacid pathway contributes to carbon source-dependent expression of the *Acinetobacter* sp strain ADP1 *pobA* gene. *Appl. Environ. Microbiol.* **69**, 1598–1606 (2003).
66. Arias-Barrau, E. *et al.* The homogentisate pathway: a central catabolic pathway involved in the degradation of L-phenylalanine, L-tyrosine, and 3-hydroxyphenylacetate in *Pseudomonas putida*. *J. Bacteriol.* **186**, 5062–5077 (2004).
67. Lee, S. Y., Park, S., Oh, T. K. & Yoon, J. H. *Celeribacter baekdonensis* sp. nov., isolated from seawater, and emended description of the genus *Celeribacter* Ivanova *et al.* 2010. *Int. J. Syst. Evol. Microbiol.* **62**, 1359–1364 (2012).
68. Ausubel, F. M. *et al.* *Short Protocols in Molecular Biology: A Compendium of Methods from Current Protocols in Molecular Biology* (Wiley, New York, 2002).
69. Bentley, D. R. *et al.* Accurate whole human genome sequencing using reversible terminator chemistry. *Nature* **456**, 53–59 (2008).
70. Delcher, A. L., Bratke, K. A., Powers, E. C. & Salzberg, S. L. Identifying bacterial genes and endosymbiont DNA with Glimmer. *Bioinformatics* **23**, 673–679 (2007).
71. Fukao, M. *et al.* Genomic analysis by deep sequencing of the probiotic *Lactobacillus brevis* KB290 harboring nine plasmids reveals genomic stability. *PLoS ONE* **8**, e60521 (2013).
72. Marx, C. J. & Lidstrom, M. E. Broad-host-range *cre-lox* system for antibiotic marker recycling in gram-negative bacteria. *Biotechniques* **33**, 1062–1067 (2002).
73. Denev, V. J. *et al.* Genetic and genomic insights into the role of benzoate-catabolic pathway redundancy in *Burkholderia xenovorans* LB400. *Appl. Environ. Microbiol.* **72**, 585–595 (2006).



74. Liu, C. & Shao, Z. *Alcanivorax dieselolei* sp. nov., a novel alkane-degrading bacterium isolated from sea water and deep-sea sediment. *Int. J. Syst. Evol. Microbiol.* **55**, 1181–1186 (2005).

Acknowledgments

This work was financially supported by COMRA program (No. DY125-15-R-01), Public Welfare Project of SOA (201005032), National Natural Science Foundation of China (41176154/41276005) and National Infrastructure of Microbial Resources of China (No. NIMR-2014-9). We thank Dr. Shicheng CHEN for providing us strain *Escherichia coli* WM3064 and plasmid pJK100, and thank Dr. Mohamed JEBBAR for critical reading of this manuscript.

Author contributions

Z.S. conceived the project and supervised the genomic and bioinformatics studies. J.C., Q.L., J.Y. and Z.S. performed the experiments and analyzed the data. J.C., Q.L. and Z.S. wrote the paper.

Additional information

Accession codes: The sequences of the six replicons of strain P73^T have been deposited in GenBank (Accession: CP004393 – CP004398). The whole genome shotgun sequence of strain B30 is also available (Accession: AMRK00000000).

Supplementary information accompanies this paper at <http://www.nature.com/scientificreports>

Competing financial interests: The authors declare no competing financial interests.

How to cite this article: Cao, J., Lai, Q., Yuan, J. & Shao, Z. Genomic and metabolic analysis of fluoranthene degradation pathway in *Celeribacter indicus* P73^T. *Sci. Rep.* **5**, 7741; DOI:10.1038/srep07741 (2015).



This work is licensed under a Creative Commons Attribution-NonCommercial-ShareAlike 4.0 International License. The images or other third party material in this article are included in the article's Creative Commons license, unless indicated otherwise in the credit line; if the material is not included under the Creative Commons license, users will need to obtain permission from the license holder in order to reproduce the material. To view a copy of this license, visit <http://creativecommons.org/licenses/by-nc-sa/4.0/>